Preparation and Physicochemical Characterization of Atorvastatin Choline Salt and its Potential for Transdermal Permeation*

Ruba T. Tarawneh**[1], Randa SH. Mansour[2], Dina El-Sabawi[1] and Imad I. Hamdan[1]

[1] School of Pharmacy, The University of Jordan, Amman, Jordan
[2] School of Pharmacy, Philadelphia University, Amman, Jordan.

ABSTRACT

Atorvastatin calcium (ATV) is an anti-hyperlipidemic agent with poor bioavailability. Several approaches were reported to improve the solubility of ATV. In this study ATV was prepared as a choline salt (ATV-C) and a complex of the prepared salt with hydroxy-propyl-beta-cyclodextrin (HPβCD) (ATV-C-CD) hoping to enhance ATV solubility, decrease the partition coefficient and improve its transdermal permeability. The pharmaceutical properties of the products were investigated. The prepared salts were characterized by FTIR, NMR and DSC, UV and HPLC. 2D NMR was successfully employed to unequivocally assign the protons of ATV, which was essential for better understanding of the structure of the formed salt. ATV-C showed higher solubility in phosphate buffer than ATV. Its log Po/phosphate buffer was found to be 1.1 while that for ATV 1.78. This change had an effect on the transdermal permeation where the ATV-C compound achieved a 4 times greater diffusion compared to ATV. Interestingly, ATV-C seemed to cause a tighter fitting of the drug into the HPβCD cavity leading to higher binding constant. However, the ATV-C-CD complex showed a negative effect on transdermal permeation.

Keywords: atorvastatin, bioavailability, transdermal, Log P.

INTRODUCTION

Atorvastatin calcium (ATV) is a statin anti-hyperlipdimic medication [1-4]. ATV reduces blood levels of LDL cholesterol and triglycerides but increases levels of HDL-cholesterol to a certain extent [5]. ATV is believed to be the most efficient and frequently prescribed medicine used to treat hypercholesterolemia [6] and prevent cardiovascular diseases [7]. As an acid with major lipophilic substituents it is insoluble in aqueous solutions at pH values less than 4; very slightly soluble in phosphate buffer of pH 7.4[8, 9]. The drug has a very low bioavailability of 12% [2, 7] which is mainly attributed to its low aqueous solubility (0.1 mg/ml) and its crystalline nature [2]. It has a half-life of 14h and undergoes hepatic metabolism [7]. The remaining unabsorbed amount of the drug shows adverse effects which is undesirable for patients [10, 11].

Several approaches for improving the solubility of poorly water-soluble drugs have been reported [12]. Salt formation [13] represents such a successful approach that leads to changing the physicochemical properties of the drug without changing its chemical structure [14]. Complexation with cyclodextrins, is yet another approach by which the solubility of several poorly water soluble drugs, such as ATV, has been improved [15-17]. Hydroxy-propyl-beta-cyclodextrin (HPβCD), is a more water soluble derivative of β-cyclodextrin, and has been more frequently used to improve the water solubility of poorly water soluble drugs [16, 18].

* This research was supported by a grant from the Deanship of Scientific Research at the University of Jordan, Amman, Jordan.
** r.tarawneh@ju.edu.jo
Received on 23/4/2019 and Accepted for Publication on 6/1/2020.

Transdermal delivery ranks now as one of the most successful innovative research area in drug delivery [19]. It has a number of advantages such as controlled delivery of the drug, avoiding first pass hepatic metabolism [20] and reducing systemic side effects [21]. Previous attempts have been made to study the transdermal permeation of ATV as an alternative for oral route administration [20-25]. Various techniques have been used to prepare transdermal patches loaded with ATV and have achieved improved transdermal permeation, an increase in bioavailability [20, 22-24]. It was also reported that transdermal delivery of atorvastatin had eliminated the increase in rat liver enzyme activity [22]. Transdermal permeation of ATV has also been improved in the presence of different permeation enhancers [20-21]. Some reports have also studied transdermal permeation of ATV as a pro-drug [25]. To the best of our knowledge, no studies involving formation of salts of ATV with organic bases have been reported.

This study aims at preparing an organic salt of ATV with choline (ATV-C), which is expected to possess enhanced solubility, lower melting temperature (lower crystallinity) and an optimized partition coefficient. These properties might have a positive influence on the transdermal delivery of ATV. ATV-C was also examined as a complex with HPβCD (ATV-C-CD), since HPβCD complexes have been reported to improve transdermal permeation of drugs [25].

1. METHODS

1.1. Materials and Equipment:

ATV was provided by JPM, Jordan with purity of > 98.5%. Choline hydroxylamine and hydroxypropyl β–cyclodextrin (HPβCD) were purchased from Sigma-Aldrich, Japan. HPLC grade methanol and acetonitrile were purchased from Tidea®. Potassium monobasic phosphate and trypsin (from porcine pancreas, lyophilized powder, 1000-2000 BAEE units/mg solid) and celloulose membrane (MWCO 9000) were purchased from Sigma-Aldrich, USA. Snakeskin dialysis tubing (MWCO 3500) was purchased from Thermo Scientific, USA. Column C8 (Equisil BDS C8, 5 µm, 250 x 4.6mm) was purchased from Dr. Maisch GmbH , Germany.

Infrared spectrophotometer used was FTIR, 8400S, Shimadzo Corporation, Japan. NMR spectrophotometer was (Bruker 500 MHz – Avance III). Differential scanning calorimeter DSC 823^e, Mettler Toledo. UV spectrophotometer Aquaris, Cecil, CE7400series, UK. Shimadzo HPLC system (LC-2010AHT) equipped with an autosampler, degasser and column temperature controller was employed for analysis. The system was also equipped with LC solution software which was used for data analysis and reporting. *In-vitro* diffusion studies were performed using standard jacketed Franz diffusion cells that were obtained from PermeGear Inc., USA.

1.2. Sample Preparation:

1.2.1. Preparation of Atorvastatin – Choline salt (ATV-C):

A sample of 1g of atorvastatin calcium was dissolved in 250 mL methanol, and then 250 mL water was added. Choline was introduced to the previously obtained atorvastatin solution in a ratio of 2:1 (choline: atorvastatin). Three hours later it was filtered and the clear filtrate which gradually turned turbid was left under the fume hood at room temperature until the solvent completely evaporated. The sample turned into a sticky opaque viscous material and was placed in a dessicator for 72 h.

1.2.2. Preparation of Atorvastatin – Choline-HPβCD Complex (ATV-C-CD):

A sample of 700 mg of HPβCD was dissolved in 200 mL distilled water and added to a solution of 453 mg of ATV-C in minimal volume of 50% aqueous methanol. It was left under the fume hood until it completely evaporated. The crystalline residue was collected and placed in a desiccator for 24 h. The product was yellowish in color.

1.3. Spectroscopic Characterization

Samples of ATV, ATV-C, ATV-C-CD, choline and HPβCD were analyzed by FTIR spectrophotometer in the

range from 4000 to 400 cm^{-1}.

^{1}H NMR spectra were obtained for samples of ATV, ATV-C, ATV-C-CD, ATV-CD mixture, choline and HPβCD. Deutrated dimethyl sulfoxide (DMSO) was used as a suitable NMR solvent.

Solutions of ATV and ATV-C in water and 50 mM phosphate buffer, pH 6.8 were prepared in the concentration range of 0.5-100 µg/mL. ATV-C-CD solutions in 50 mM phosphate buffer were also prepared in the concentration range of (5-75) µg/mL. The solutions were scanned in the range of 200-350 nm. The absorbance values were also recorded for the solutions at 240 nm.

1.4. Differential Scanning Calorimetry (DSC)

Thermal characteristics of ATV, ATV-C product and ATV-C-CD complex were studied using differential scanning colorimetery. The samples were hermetically sealed in aluminum pans and heated at a constant rate of 10°C/min over a temperature range of 25 to 250 °C. Inert atmosphere was maintained by purging nitrogen gas at flow rate of 80 mL/min. An empty aluminum pan was used as a reference.

1.5. Quantitative Analysis by HPLC

The employed HPLC method for quantitative determination of ATV-C was based on a previously published and validated method with some modifications [27]. Briefly, the method employed a C8 column and a mobile phase composed of acetonitrile: 20 mM phosphate buffer (55:45), pH 4, with a flow rate of 1 mL/min. Injection volume was 100 µL with detection at 240 nm. A stock solution of 1 mg/mL ATV in methanol was prepared, from which calibration curve solutions were made in the range (0.25-50) µg/mL using 50 mM phosphate buffer, pH 6.8.

For determination of ATV in skin permeation experiments, the method was slightly modified by employing a gradient system where the mobile phase consisted of acetonitrile: 20 mM phosphate buffer (55:45), pH 4 for 9 min then acetonitrile percentage was increased to 70% for 3 minutes then back to 55% for 5 min. Nevertheless, the method was fully validated for selectivity, precision, accuracy and linearity with satisfactory results.

Selectivity was established by demonstrating that neither buffer components, choline nor stratum corneum constituents eluted at the same retention time of ATV. Linearity was satisfactory with $R^2 > 0.999$ for concentrations in the range (0.25 – 50) µg/mL ATV.

Typical calibration equations for the isocratic and gradient methods were Y= 56.59 X + 9.094 and Y= 211538 X - 55005, with correlation coefficients of 0.9998 and 0.9992 respectively.

For precision, 5 samples of ATV were prepared at low (0.25 µg/mL), intermediate (10 µg/mL) and high (50 µg/mL) concentration levels. The obtained RSD values were (0.34), (0.41) and (0.82) and thus concluded highly satisfactory.

Sensitivity was assessed by preparing increasingly low standard concentrations of ATV. Back calculations were carried out to determine their concentrations using the obtained linear equation. The RSD value was assessed at each concentration level. The lowest concentration that provided a RSD value < 1 was 0.25 µglmL. This value was adopted as the lowest limit of quantification (LOQ).

For assessment of accuracy, 5 standard samples were prepared at low (0.25 µg/mL), intermediate (10 µg/mL) and high (50 µg/mL) concentrations. Back calculations were performed using the obtained calibration equation. The average percentage difference between their nominal concentrations and their calculated values were reported and assessed. At all concentration levels the percentage difference was < 1% and thus the method was concluded sufficiently accurate.

1.6. Solubility and Apparent Partition Coefficient

Solubility test was performed according to shake flask method [28]. Excess amount of ATV, ATV-C and ATV-C-CD were placed in eppendorf tubes (three samples for each) and 1 mL of 50 mM phosphate buffer, pH 6.8 was added. The samples were then placed on a shaker set at

37°C, 150 rpm for 24 h. Samples were centrifuged at $15x10^3$ rpm for 15 min. The clear supernatant was collected and properly diluted and injected onto HPLC system as described in Section 2.5.

To determine the partition coefficient, 0.5 mL of the previously collected supernatant was placed in a new Eppendorf tube and 0.5 mL of n-octanol was added. The samples were placed on a shaker at 37°C, 150rpm for 24 h. The samples were centrifuged at $15x10^3$ rpm for 15 min and then the aqueous layer was injected onto HPLC as described in section 2.5 and properly diluted when required. Log partition coefficient was determined according to Equation 1.

$$\text{Log } P_{o/aq} = \log [(S_o - C_{aq}) / (C_{aq})] \quad \text{Equation 1}$$

Where S_o is the experimentally determined saturated solubility of ATV in 50 mM phosphate buffer pH 6.8 and C_{aq} is the experimentally determined concentration of ATV in the aqueous phosphate buffer layer after adding 1-octanol.

1.7. Phase Solubility and Binding Constant

A series of eight solutions of HPβCD in the range of 0-20 mM were prepared in phosphate buffer, pH 6.8. To separate eppendorf tubes containing excess amount of either ATV (3.5 mg) of ATV-C (3.5 mg), 1 mL of each of the HPβCD solutions was added. Solutions were shaken for 24 h at 37 °C (150 rpm), centrifuged at 9000 rpm for 20 min and the supernatant was collected, diluted properly and injected onto HPLC. The binding constant was calculated using the slope of the obtained phase solubility diagram [29]:

$$K = \text{Slope} / S_0 (1\text{-slope}) \quad \text{Equation 2}$$

Where S_0 is the concentration of ATV in 50 mM phosphate buffer, pH 6.8.

1.8. *In-Vitro* diffusion studies

Human skin from abdominal plastic surgery was obtained from a local hospital immediately after the surgery. The skin donor was a 40 years old female and her approval was granted after the research objective was explained to her.

Punched skin discs of 25 mm diameter were placed in petri dish with SC side up and 1% w/v trypsin was added until the skin surface is totally immersed. The petri dish was then occlusively covered and incubated at 32°C for 24-48 h until the separation of the SC was evident. The separated SC sheets were rinsed several times with distilled water.

All test suspensions for ATV, ATV-C and ATV-C-CD were prepared in 50 mM phosphate buffer, pH=6.8 at 110% of the solubility concentration. The ATV-CD suspension was prepared by mixing 140 mg of HPβCD and 52 mg of ATV in 20 mL phosphate buffer where a milky suspension formed.

In-vitro diffusion studies were performed using stirred Franz diffusion cells of 1 cm^2 diffusion area and 8 mL receiver compartment volume. The SC sheets were separated and washed, gently pressed by a filter paper and soaked in phosphate buffer, pH 6.8 for 30 min before use. The cells were jacketed with circulating water maintained at 32°C. The receiver compartment was filled with phosphate buffer, pH 6.8 previously filtered by 0.45 µm nylon filter and equilibrated at 32°C. After visually checking its integrity, a SC sheet was placed on a piece of cellulose membrane previously soaked in phosphate buffer, pH 6.8 and then mounted on the top of the receiver compartment. Special care was provided to prevent air bubbles entrapment under the membrane or between the membrane and the SC. The donor compartment was then placed and fastened by a clamp. 1 mL of the test suspension was placed in the donar compartment. The compartment was examined visually to make sure no air bubbles formed on the suspension side. The donor and the side arm were then occlusively covered by parafilm and the cells were stirred at 32°C for 24-26 h. At specified time intervals (0.25, 0.5, 1, 2, 3, 5, 7, 12, 24 and 26 h) , 0.5 mL of the receiver buffer was withdrawn and immediately replaced with an equal volume of fresh buffer previously filtered by 0.45 µm nylon filter and equilibrated at 32°C.

The experiments were performed as 4-6 replicates.

The withdrawn samples were injected onto the gradient HPLC system described in Section 2.5. The diffusion profiles were constructed by plotting the average cumulative diffused amount (μg/mL/cm^2) versus time (h).

1.9. Diffusion across a synthetic membrane

Test suspensions were prepared in the same manner as described in Section 2.8. The suspensions were tested using the same diffusion cells system described in the previous section. The cells were filled with 50mM phosphate buffer, pH 6.8 in the receiver compartment and 1 mL of the test suspension in the donar compartment. Cellulose membranes with cutoff values of 3.5 or 9 kDa were used. Samples were withdrawn from the receiving compartment at 0.5, 2, 4, 6, 24, 27, 30 and 48 h.

The withdrawn sample was replaced with phosphate buffer. Solutions were diluted as required and ATV content was determined by HPLC. The diffusion profiles were constructed by plotting the average cumulative diffused amount (μg/mL/cm^2) versus time (h).

2. RESULTS AND DISCUSSION

2.1. Characterization of ATV-C salt:

The FTIR spectra obtained for ATV, Figure 2a, exhibited major peaks at 1675, 2875, 3240, and 3510 cm^{-1} corresponding to C=O stretching, C-H stretching, NH stretching and OH stretching respectively. The spectra were generally in agreement with previously reported spectra for ATV [13]. In comparison, the FTIR spectrum of ATV-C, Figure 2a, showed a slight shift in the mentioned peaks. They showed at 1645, 2948, 3231 and 3349 cm^{-1} for C=O stretching, C-H stretching, NH stretching and OH stretching respectively. A reduction of the carbonyl frequency by 30 cm^{-1} suggests a significant weakening of the carbonyl double bond due to salt formation between the negatively charged carboxyl and the electron deficient positively charged quaternary amine group of choline. However, the most obvious change was the appearance of a huge peak in the hydroxyl bond region ≈ 3000 – 3500 cm^{-1} similar to that of the native choline, indicating the presence of choline in the salt and the heavy involvement of hydrogen bond formation. Spectra for the ATV-C-CD complex, Figure 2b, also showed peaks at 1645 referring to C=O stretching, in addition to the peaks at 2885 and 3248 cm^{-1} corresponding to C-H stretching and OH stretching respectively. The most characteristic feature of ATV-C-CD spectrum was the low intensity of all the peaks which might be attributed to the molecule being included within the HPβCD cavity. No new peaks appeared in the spectra of the inclusion complex indicating no chemical bonds were involved in the complex formation.

Stronger evidence of ATV-C salt formation was obtained by NMR. H^1 NMR spectra of ATV, ATV-C, ATV-C-CD and ATV-CD were obtained in DMSO. They were used to study the formation of ATV-C and ATV-C-CD. The spectra of ATV agreed with those previously reported [30-31]. Chemical shift data for the relevant spectra are summarized in Table 2. The change in chemical shift of the various protons on the products (ATV-C, ATV-C-CD) compared to ATV are also shown between brackets. Accordingly, aromatic protons of ATV-C barely showed changes in their chemical shifts. On the other hand, the amide protons and aliphatic side chain protons showed more detectable shifts with the maximum being for protons 2 and 4 (attached to the carbons bearing the hydroxyl group) which suggest perturbation of intermolecular hydrogen bonding involving these OH groups in ATV. However, peak assignment for proton NMR spectra of ATV appeared to be conflicting in relevant literature [30, 32]. Therefore, detailed 2D NMR spectral experiments including DEPT135, COSY and HMQC were undertaken with the purpose of obtaining unequivocal assignments of ATV protons. Figure 3 shows the most relevant 2D NMR measurements. Starting from the DEPT NMR there was only 3 -CH- carbons, two of which appear to resonate at the same frequency at about δ 69. The other one appears at a higher field about δ 25. Thus the signal of the two carbons at δ 69 was assigned for the two –CH- carbons bearing the hydroxyl groups (2+4) and the one at δ 25 was

assigned for the CH bearing the methyl groups (C7) based on the chemical shift values. According to Figure 3a, C7 correlates only with the proton signal (multiplet) at δ 3.19 which confirms that the signal corresponds to CH (7). For the two CH carbons at about δ 69 they correlate with proton signals at δ 3.45 and 3.7, thus those signals must be due to CH protons 2 and 4. The remaining aliphatic signals, therefore, must be related to protons of CH_2 groups which appear in the DEPT spectrum in the range 40-50 ppm.

Thus, from their correlation in Figure 3a, it could be confirmed that the signals at δ of 1.19- 1.33, 1.87-1.99 and 3.72-3.9 must belong to those protons of CH_2 groups. Careful examination of Figure 3b revealed that the signal at δ 1.87-1.99 was the one (of the mentioned signals) that correlates clearly with only a CH proton (at δ 3.69) and thus it must be due to the two protons on C1. It follows, from that on the rest of correlations in Figure 3b that the signal at δ 3.69 must be due to proton number 2 and since it also correlates with the CH_2 signal at about δ 1.19 the latter must be due to proton number 3 which also correlates with the CH signal at δ 3.48 which must be due to proton number 4. Following the same pattern of correlations the protons number 5 and 6 must be related to signals at δ 1.5 and 3.72-3.90 respectively.

Our ^{1}H NMR spectral assignments is consistent with only that reported by Galiullina et al., 2018. However, this is the first report of detailed proton assignment of ATV based on 2D NMR spectroscopic studies that confirms the chemical shifts for each of the aliphatic side chain protons on ATV. It was interesting to observe that each of the CH_2 protons on the side chain were unexpectedly non-equivalent and spin couple with each other, which supports the suggestion that the side chain adopts a rather rigid conformation. Therefore, the effect of the choline-ATV salt formation on proton chemical shifts can now confidently be addressed. Accordingly, the most seriously shifted signal (to a lower frequency) was that corresponding to protons on C1 followed by C2 and C3 (Figure 4) which accords very well with the proton on carboxyl being replaced by the more electron rich amino group of choline. Most importantly however, was the confirmation of the presence of protons of both of choline and ATV in the spectrum of the salt. Moreover, when the integrated peak area of the ATV protons at δ = 1.33ppm, the two methyl protons) was divided by that of choline (at δ = 3.8ppm, CH_2 *- N) a ratio of 3:1 was obtained which accords with 1:1 salt formation between ATV and choline. Concerning protons of choline hydroxide, the two protons on CH_2 attached to O were shifted to a lower frequency but those attached to the N exhibited a more dramatic shift to higher frequency, in accordance with salt formation through interaction between the positively charged nitrogen and the negatively charged carboxyl group of the ATV. In this process, the hydroxide anion is replaced by the carboxylate group; consequently the electron shield provided by the hydroxyl would become less intense leading to shifts towards higher frequency for the relevant protons.

Chemical shift of the OH group in choline showing at 4.66 ppm disappeared in the formed ATV-C salt and ATV-C-CD complex which suggests the significant change in hydrogen bond formation of the OH group of choline during formation of salt. For ATV, the amide proton at 9.78 was shifted in ATV-C to 9.86 suggesting heavier involvement in hydrogen bond formation most probably with the OH of the chain.

However, the obtained NMR spectra for ATV-CD were similar to ATV and those for ATV-C-CD were similar to ATV-C, which indicate that either binding of ATV or ATV-C to HPβCD might not result in a significant shift in proton NMR frequencies or they simply do not bind in DMSO (NMR solvent).

The DSC profile of ATV (Figure 5) was consistent with those previously reported [33-34] showing a broad endotherm at around 90°C that corresponds to loss of water molecules, an endotherm at 155.7°C, that corresponds to the melting of ATV and another

endothermic peak at 228°C that is due to a phase transition with potential degradation [30, 35-36]. For ATV-C, Figure 6, the DSC profiles showed an endotherm at 78.7°C indicating water loss and another sharp good size endothermic peak at 102°C that was most likely due to the melting of ATV-C. Although significantly reduced in intensity the characteristic peak corresponding to phase transition with potential degradation for ATV (at ≈220°C) also appeared in the DSC thermogram of ATV-C. However, there was no peak corresponding to the melting point of ATV in the thermogram which supported the involvement of all the ATV in salt formation.

The DSC profile of ATV-C-CD, Figure 5, shows a broad endothermic peak at 78.7 reflecting a loss of water similar to that in ATV and ATV-C. A less intense peak at 104.3 that is most likely due to melting of ATV-C. In addition, another event appeared at 223 and 243 °C which was characteristic for potential degradation of ATV, while in the region where ATV melting point is supposed to appear there was no peak in the thermogram of the complex which indicated the formation of the inclusion complex. Therefore, it is likely that ATV-C did not exist simply as a separate entity in the presence of HPβCD. It appears that ATV-C forms an inclusion complex with HPβCD, which results in different thermal behavior and possibly other physicochemical properties from that of ATV-C.

Solutions of ATV and ATV-C were prepared in 50 mM phosphate buffer, pH 6.8, in the concentration range of (0.5-100) µg/mL. They were scanned by UV spectrophotometer in the wavelength range of 200-350 nm. Plots of absorbance at 240 nm versus concentration were then obtained. Only absorbance values that were in the linear range were included, which corresponded to the concentration range (5-20) µg/mL. The calibration equation for ATV and ATV-C in phosphate buffer, pH 6.8 are $Y = 0.0405 X - 0.003$, $R^2 = 1$ and $Y = 0.0294 X + 0.0355$, $R^2 = 0.998$, respectively. Obviously, two different slopes for the calibration equations for ATV and ATV-C were obtained reflecting the lower content of ATV in ATV-C. Moreover, when a sample of ATV-C was dissolved in phosphate buffer to have a final concentration of 12.5 mg/mL an absorbance value of 0.398 was obtained which resulted in a calculated concentration of 9.91 µg/mL when calculated based on the calibration curve equation of ATV. Thus the percentage of ATV found in the taken sample of ATV-C corresponds to ≈ 80% which is close to the hypothetical percentage (84%) assuming a 1:1 salt formation ratio between ATV and choline. The slight discrepancy between the actual and the theoretical percentage could be attributed, at least in part, to residual water or to excess choline content.

ATV-C-CD was prepared in 50 mM phosphate buffer, pH 6.8 in concentration ranges of (4.5-75) µg/mL. The solutions were scanned in the wavelength range 200-350 nm. From the obtained UV spectra; we observed a shift in λ_{max} from 243 nm in case of ATV-C to 253 nm in ATV-C-CD (Figure 6) which suggested association and dissociation of ATV-C-CD complex at high and low concentration of the complex respectively.

Solutions of ATV were prepared in 50mM phosphate buffer, pH 6.8 in the concentration range of 0.25-50 µg/mL. The samples were analyzed using HPLC conditions described in quantitative analysis by HPLC. A representative calibration equation could be given by: $y = 211538 x - 55005$, $R^2 = 0.9992$ and was used for the determination of ATV-C in various characterization experiments including solubility and partition coefficient measurements.

2.2. Solubility and apparent partition coefficient (PC)

Solubility was determined for ATV, ATV-C and ATV-C-CD in 50 mM phosphate buffer pH 6.8 (Table 3) and was expressed in terms of ATV content. Solubility obtained for ATV (0.26 mg/mL) was comparable to previously reported values [2, 30]. The solubility of ATV-C was found to be two times greater than the solubility of ATV. When HPβCD complexed with ATV-C, it appeared

to increase the solubility of ATV even further reaching about 1.8 mg/mL. This was almost 8 times the solubility of native ATV. Although previous reports have studied the interaction between ATV and HPβCD and all of them reported increase in solubility of ATV as a result of complexation with HPβCD. The maximum reported increase for (1:1) ATV-C: HPβCD complex was less than 3 folds [16, 30, 37].

The best candidates for transdermal diffusion have to combine a number of criteria. They should have a high but balanced PC, low melting point, molecular weight less than 600 Da which is related to solubility [38].The obtained apparent PC and Log $P_{o/aq}$ values were determined and are shown in Table 4. The obtained Log P for ATV (1.86) was comparable to that previously reported [39]. The results showed that the choline salt and the HPβCD had lower apparent PC than ATV. ATV-C and ATV-C-CD exhibited almost one fifth and one half the value of PC for ATV, respectively. This was anticipated to be advantageous to transdermal permeation, as PC value became closer to the generally recommended optimum range. It was interesting that while the aqueous solubility of ATV-C-CD was four times that of ATV-C, its PC value was also 3 times higher than that of ATV-C. An explanation could be that HPβCD provides an escape place for the hydrophobic ATV-C in absence of organic phase; however, in presence of the organic phase the drug dissociates from HPβCD and diffuses to the organic solvent.

2.3. Phase solubility study

Stability constants (K) were calculated from the phase solubility diagram (PSD), Figure 7, which were obtained according to a well-established method described by Higuchi and Connors, 1965 [29]. K values were found to be 74 M^{-1} and 119 M^{-1} for ATV and ATV-C respectively in the range of 0-20 mM HPβCD i.e. K almost doubled for ATV-C compared to ATV. When comparing the solubility of these two components at the maximal concentration of tested HPβCD we found that ATV-C resulted in more than three times increase in solubility of ATV. Therefore, either of the approaches: choline salt formation or inclusion into HPβCD, resulted in almost doubling the solubility of ATV (from 266 to ≈ 633 µg/mL) at maximal HPβCD concentration.

However, in case of ATV-C, HPβCD results in more than four times increase in solubility of ATV, which suggested that the observed increase in solubility of ATV in that case did not simply result from the additive effect of solubility enhancement of each of the HPβCD and choline individually i.e. synergistic effect of enhanced solubility. Together with the observed almost doubling effect for K value of ATV-C compared to ATV, this has led to a conclusion that the presence of choline with ATV (ATV-C) resulted in a better fitting of the drug (ATV) with the cavity of HPβCD.

2.4. Diffusion across human skin

It is well accepted that human skin is the best and most relevant type of barrier for *in-vitro* diffusion testing [40]. In this study we considered using human stratum corneum as the diffusion barrier in the in-vitro diffusion studies. Cumulative diffused amount of drug was plotted in each case against time (Figure 8a). Figure 8a shows that diffusion of ATV-C through human skin was four times higher than that of ATV and reached about 6 µg/mL/cm^2.

The significant four time increase in the diffusion of ATV could be attributed to achieving optimum PC value of ATV when in salt form with choline. As previous reports have advocated the use of cyclodextrin as an excipient that facilitates transdermal permeation of some drugs [41], it was decided to be tested with ATV-C in effort for even further transdermal permeation. Surprisingly, the diffused amounts was lowest when HPβCD exists along with ATV-C (as the complex ATV-C-CD); even less than that of the native ATV. The observed negative effect of HPβCD on transdermal permeation of ATV was less likely to be attributed to the hydrophilic-lipophilic balance because the complex exhibited much higher solubility than ATV-C while maintaining a favorable PC value (Table 3). Therefore, other factors such as the molecular size and

stability constant of the complex must be considered. According to the results obtained it seemed that the presence of choline resulted in higher binding constant between ATV and HPβCD. Therefore, the release of ATV from HPβCD and its diffusion through skin decreased. In order to further investigate the effect of molecular size and stability constants on transdermal permeation of ATV-C, a diffusion (drug release) experiment through synthetic membranes with two different molecular mass cutoff points (3.5 and 9 kDa) was carried out. The solutions were prepared in the same manner as those used for the diffusion across human skin. The cumulative diffused amount in each case was plotted against time (Figure 8b and 8c). The overall diffused amount in case of the membrane with 9 kDa cutoff point was obviously higher than that obtained with the 3.5 kDa membrane. The difference was more noticeable in cases of ATV-C-CD which supports that the size of the complex led to significant effect on the diffusability of the complex. However, in all cases the preparations containing HPβCD showed the highest overall diffused amount which might be attributed to concentration gradient effect since the employed concentrations (saturation) was 8 and 4 times higher than that of ATV and ATV-C respectively. Comparing the results of the simple diffusion with those of transdermal permeation studies and keeping in mind that the saturated solubility concentration of relevant compounds were employed, the low transdermal permeation of ATV-C-CD observed must have been as a result of some interaction with some stratum corneum components rather than size effect. Although the effect of HPβCD was found negative pertaining immediate transdermal diffusion, it might represent an interesting option for prolonged transdermal preparation intended for very long periods of therapeutic effects.

CONCLUSION

ATV was shown to form an ion pair salt with choline leading to a lower melting point (≈102°C) which is at the border line for definition of ionic liquids. The salt was fully characterized with UV, FTIR, NMR techniques. Solubility and partition coefficients of the salt were also determined and found to be improved compared to those of ATV, where solubility increased while partition coefficient decreased to lie within the optimum range of ideal transdermally diffusing compounds. Performing diffusion experiments utilizing human skin revealed that, salt formation improved transdermal diffusability of ATV more than four times which was highly interesting and promising for development of a successful transdermal delivery system of ATV. In attempts to further evaluate the transdermal delivery of ATV, effect of HPβCD was examined. Interestingly, it appeared to bind tighter to ATV-C than ATV; however its overall effect on transdermal delivery was largely negative.

Acknowledgment

The authors wish to thank the Deanship of Scientific Research at the University of Jordan for financial support (Grant recommendation No. 66/2016/2017).

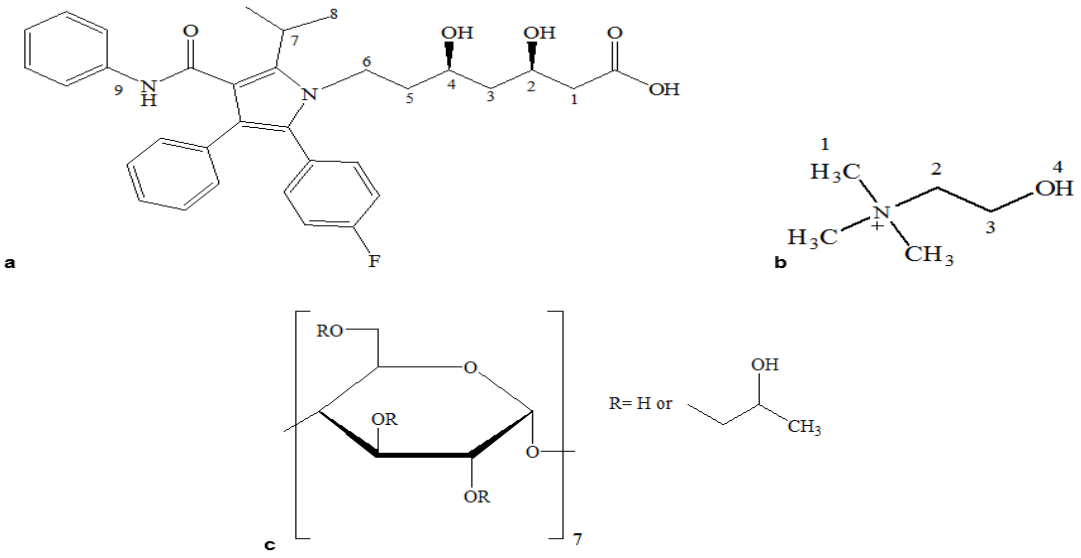

Figure 1: Chemical structure of a) ATV, b) choline and c) HPβCD

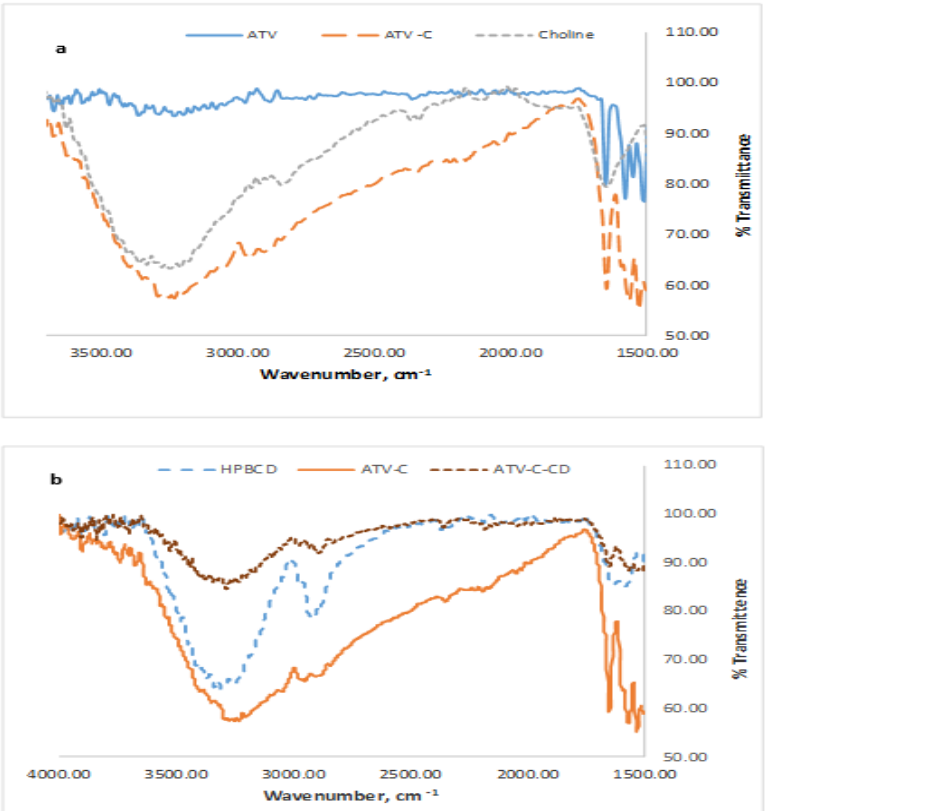

Figure 2: FTIR spectrum of a) ATV, choline and ATV-C and b) ATV-C, HPβCD and ATV-C-CD

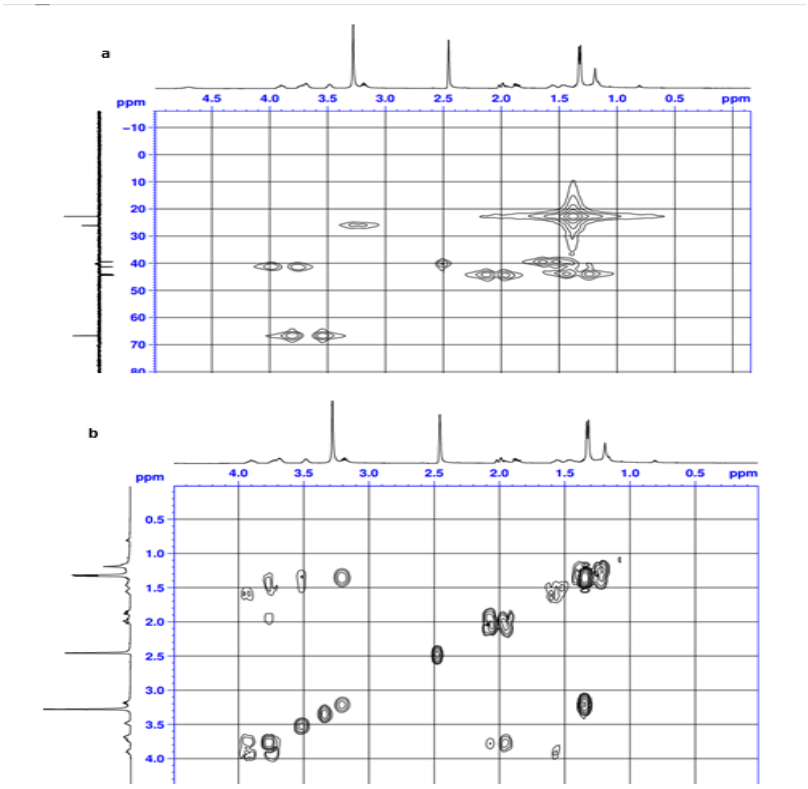

Figure 3: 2D NMR experiments for ATV: a) HMQC, b) proton NMR

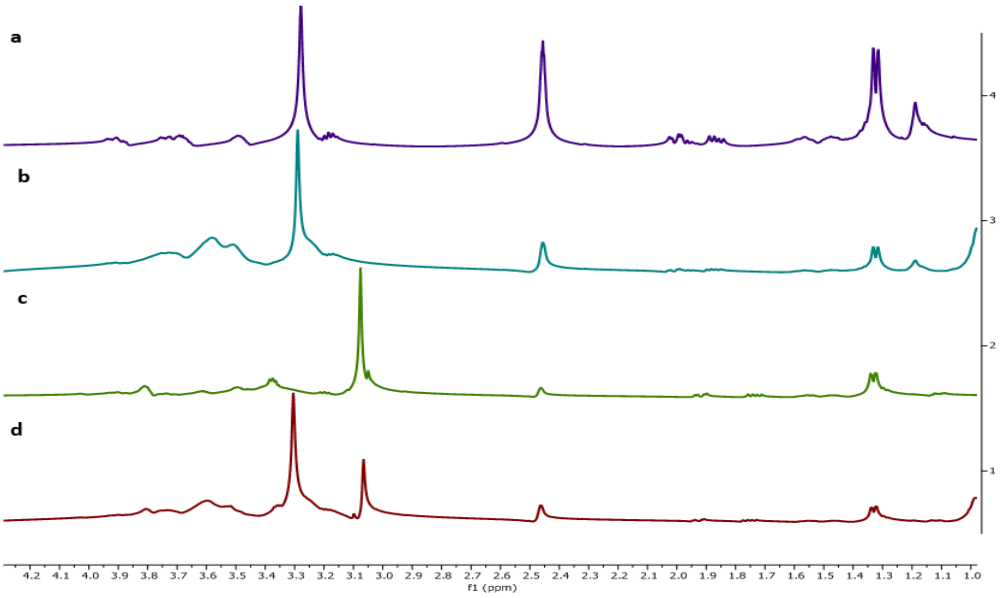

Figure 4: ^{1}H NMR spectra of: a) ATV, b) ATV-CD, c) ATV-C and d) ATV-C-CD

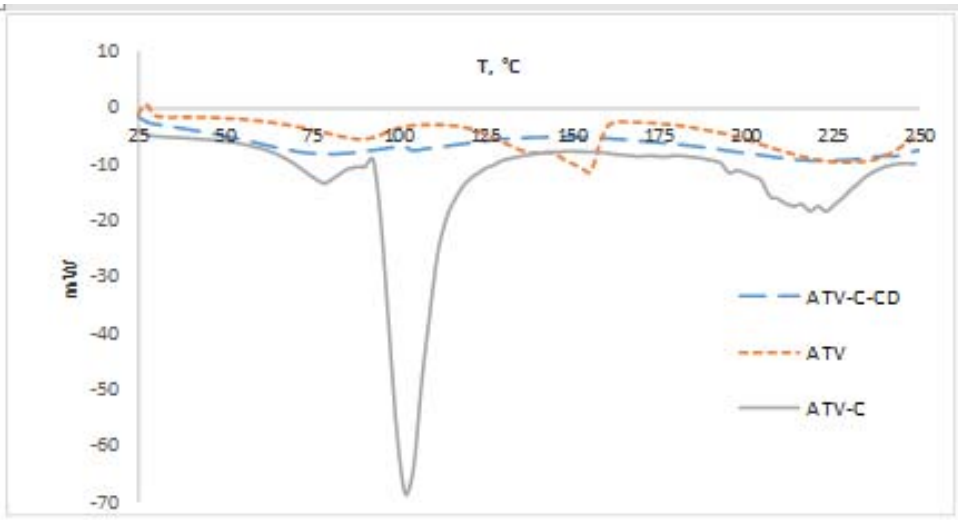

Figure 5 DSC profile of ATV, ATV-C and ATV-C-CD

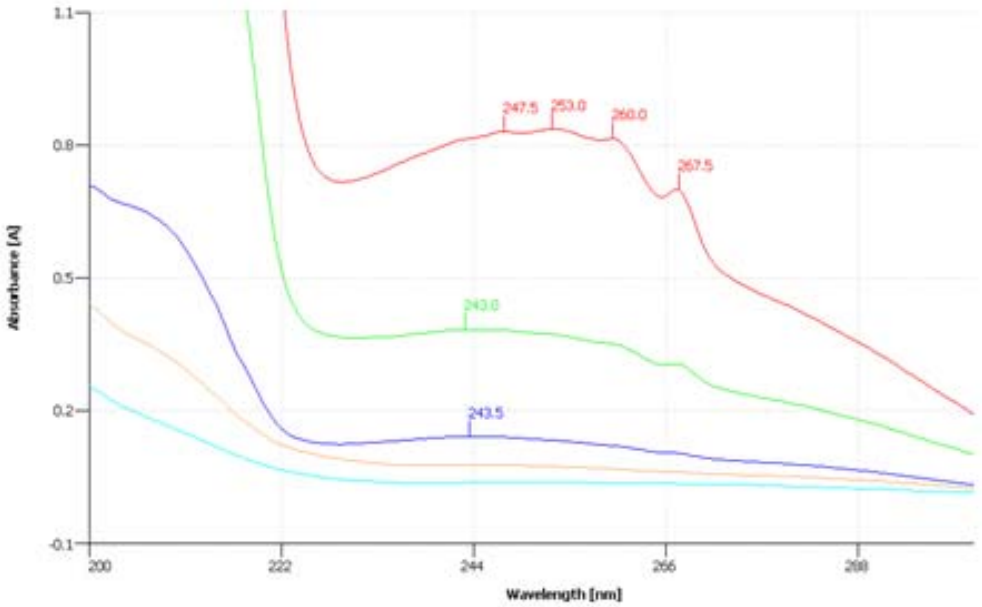

Figure 6 Overlaid UV spectra for solutions of increasing concentrations of ATV-C-CD in phosphate buffer pH = 6.8

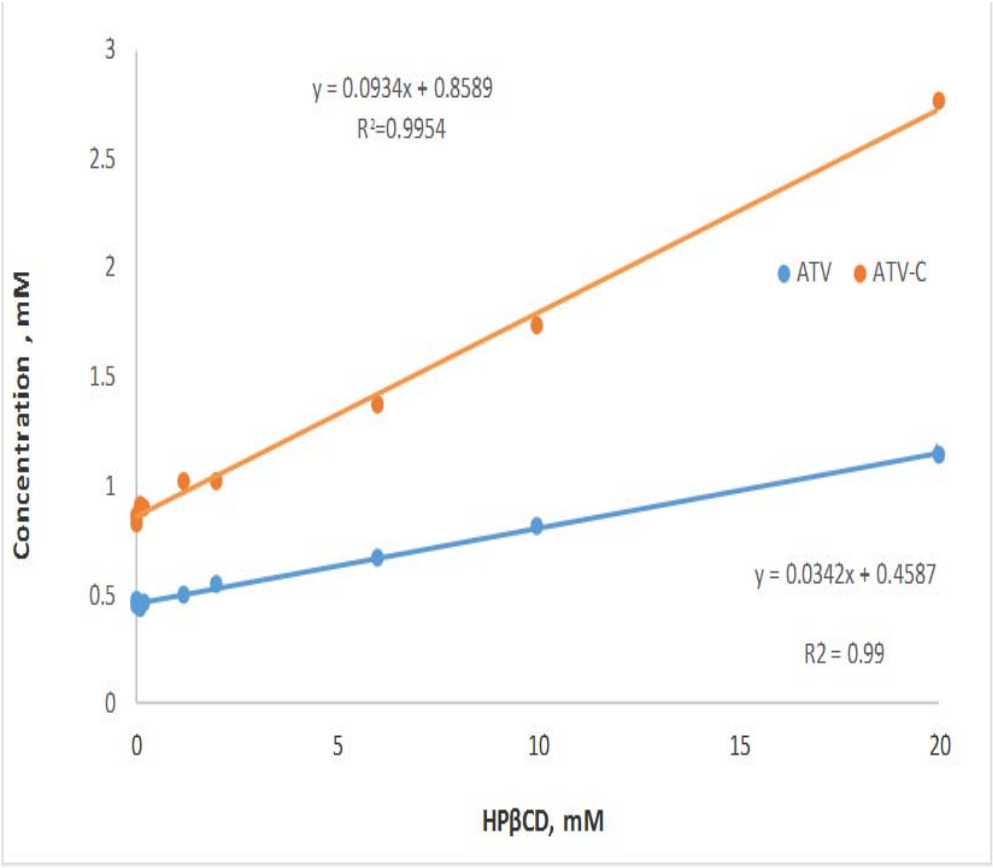

Figure 7 Phase solubility diagram of ATV or ATV-C / HPβCD

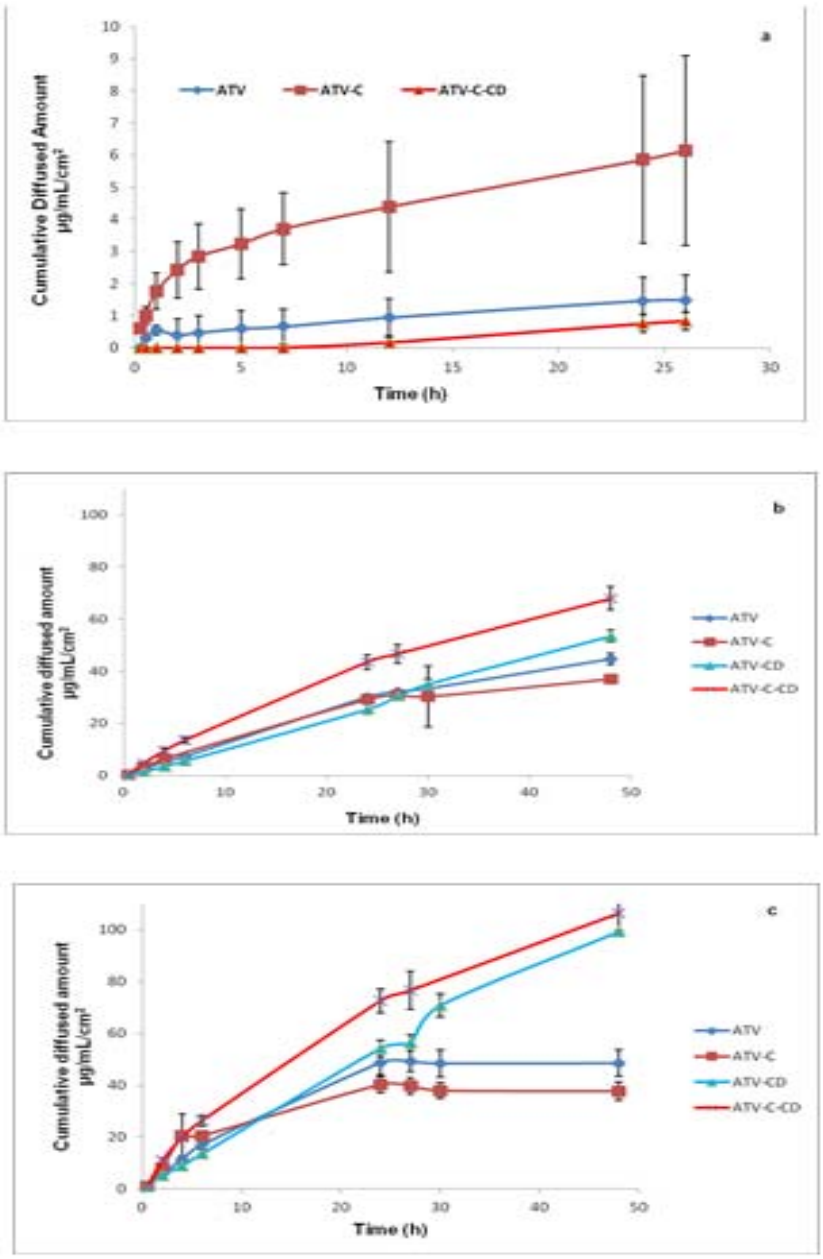

Figure 8 Diffusion of ATV and the produced compounds across a) human stratum corneum, b) a synthetic membrane with cutoff of 3.5 kDa and c) a synthetic membrane with cutoff of 9 kDa

Table 1. FTIR Data of ATV, choline, HPβCD and produced compounds obtained from spectrums

Compound	Peak (cm^{-1})	Group	Comments
ATV-C	1675	C=O	Sharp
	2875	CH stretching	
	3510.77	OH stretching	
	3240	NH stretching	
Choline	1477	CN stretching	
	1643		Broad
	2841	CH stretching	
	3243	NH stretching	
	3332.37	OH stretching	
CDX	3299	OH stretching	
	2914	CH stretching	
	1629	Weak	
ATV-C	1645	C=O	Sharp, intense
	2948	CH stretching	
	3231	OH stretching	
	3349	NH stretching	Weak
ATV-C-CD	3284.82	OH stretching	
	2885	CH stretching	
	1643	C=O	Weak

Table 2. Distinctive Chemical Shifts of ^{1}H NMR spectra of Choline, ATV, ATV-C, ATV-CD and ATV-C-CD. The change in chemical shift= chemical shift of product – chemical shift of ATV is shown in brackets.

Choline	ATV	ATV-C	ATV-CD	ATV-C-CD
3.03, H_1	1.19 +1.33, H_3 (CH_2)	1.11 + 1.33 (-0.08) (0)	1.19 + 1.33	1.11 + 1.36 (-0.08) (+0.03)
3.12, H_2	1.36, H_8 ($2CH_3$)		1.36	
3.83, H_3	1.45 + 1.55, H_5 (CH_2)	1.45 + 1.55	1.45 + 1.55	1.45 + 1.55
4.66, H_4	1.87 + 1.99, H_1 (CH_2)	1.73 + 1.92 (-0.14) (-0.07)	1.87+ 2.0 (0) (+0.01)	1.75 + 1.92 (-0.12) (-0.07)
	3.19, H_7 (CH)	3.2 (+0.01)	3.19	3.19
	3.48, H_4 (CH)	3.49 (+0.01)	3.51 (+0.02)	3.52 (+0.03)
	3.69, H_2 (CH)	3.6 (-0.09)	3.7 (+0.01)	3.59 (-0.1)
	3.72 + 3.9, H_6 (CH_2)	3.73 + 3.89 (+0.01)(-0.01)	3.71 +3.9 (-0.01) (0)	3.73 + 3.9 (+0.01) (0)
	7.46, (Aromatic H)	7.48 (+0.02)	7.46	7.47 (+ 0.01)
	9.78, H_9 (NH)	9.84 (+0.06)	9.77 (-0.01)	9.82 (+0.04)

Table 3. Solubility (µg/ml) and apparent PC and Log $P_{o/aq}$ of the ATV and related compounds in 50 mM phosphate buffer, pH 6.8.

Compound	Solubility of ATV µg/ml ± (S.D.)	Apparent PC± (S.D.)	Log $P_{o/aq}$
ATV	265 ± (2.63)	73.5 ± (2.37)	1.86
ATV-C	480.7 ± (0.4)	12.5 ± (1.07)	1.16
ATV-C-CD	1808.73 ± (141.83)	33.5 ± (2.26)	1.524

REFERENCES

1. Prajapati K.P., Bhandari A. Spectroscopic method for estimation of atorvastatin calcium in tablet dosage form. *Indo Global J. of Pharm. Sci.* 2011; 1(4): 294-299.
2. Rodde M.S., Divase G.T., Devkar T.B., and Tekade A.R. Solubility and bioavailability enhancement of poorly aqueous soluble storvastatin: *in vitro*, *ex vivo*, and *in vivo* studies. *BioMed Res. Int*. Volume 2014; 10 pages.
3. Alhazmi H.A., Alnami A.M., Arishi M.A.A., Alameer R.K. , Al Bratty M., Rehman Z. , Javed S.A. and Arbab I.A. A fast and validated reversed-phase HPLC method for simultaneous determination of simvastatin, atorvastatin, telmisartan and irbesartan in bulk drugs and tablet formulations. *Sci. Pharm*. 2018; 86, 1.
4. Alexandar S., Diwedi R. and Chandrasekar M.J.N. A RP-HPLC method for simultaneous estimation of atorvastatin and ezetimibe in pharmaceutical formulation. *Pharma Sci. Monit.* 2012; 3(3), Suppl-1: 1875-1883.
5. Wani T.A., Ahmad A., Zargar S., Khalil N.Y. and Darwish I.A. Use of response surface methodology for development of new microwell-based spectrophotometric method for determination of atorvastatin calcium in tablets. *Chem. Cent. J*. 2012; 6(134): 1-9.
6. Lea A.P., Mc Tavish D.: Atorvastatin: A review of its pharmacology and therapeutic potential in the management of hyperlipidaemias. *Drugs.* 1997; 53:828–847.
7. Ghanty S , Sadhukhan N. and Mondal A. Development and validation of a UV- spectrphotometric method for quantification of atorvastatin in tablets. *J PharmaSciTech*. 2012; 2(1): 34-40.
8. Kim J.S., Kim M.S., Park H.J., and Ji S.J. Physiological properties and oral bioavailability of amorphous atorvastatin hemi-calcium using spray drying and SAS process. *Int. J. Pharm*. 2008; vol. 359, pp. 211–219.
9. Choudhary A., Rana A.C., Aggarwal G., Kumar V., and Zakir F. Development and characterization of an atorvastatin solid dispersion formulation using skimmed milk for improved oral bioavailability. *Acta Pharm. Sin. B*. 2012; vol. 2, no. 4, pp. 421–428.
10. Jahan R., Saiful Islam M.D., Tanwir A., and Chowdhury J.A. **In vitro** dissolution study of atorvastatin binary solid dispersion. *J Adv Pharm Technol* Res. 2013; Jan-Mar; 4(1): 18–24.
11. Choudhary A., Aggarwal G., Zakir F., Kumar V. Mini review: Journey of solid dispersion technique from bench to scale. *Int Res J Pharm.* 2011; 2:46–51.
12. Saharan V.A., Kukkar V., Kataria M., Gera M., Choudhury P.K. Dissolution enhancement of drugs part II: Effect of carriers. *Int J Health Res*. 2009; 3:207–23.
13. Panghal D., Nagpal M., Thakur G.S. and Arora S. Dissolution improvement of atorvastatin calcium using modified locust bean gum by the solid dispersion technique. *Sci. Pharm*. 2014; Jan-Mar; 82(1):177-191.
14. Kim, H., Gao, J.and Burgess, D. J. Evaluation of solvent effects on protonation using NMR spectroscopy: Implication in salt formation. *Int. J. Pharm.* 2009; 377(1-2): 105–111.
15. Chiou W.L.and Riegelman S. Pharmaceutical applications of solid dispersion systems. *J Pharm Sci*. 1971; 60:1281–302.
16. Palem C.R., Dudhipala N.R., Goda S. and Pokharkar V.B. Development and optimization of atorvastatin calcium cyclodextrin inclusion complexed orally

disintegrating tablets with enhanced pharmacokinetic and pharmacodynamic profile. Int. J. Nanotechnol. 2016; 9(2): 3170-3181.

17. Chaudhary V.B. and Patel J.K. Cyclodextrin inclusion complex to enhance solubility of poorly water soluble drugs: A review. *IJPSR.* 2013; Vol. 4(1): 68-76.
18. Loftsson T., and Brewster M. E. Pharmaceutical applications of cyclodextrins. 1. drug solubilization and stabilization. *J. Pharm. Sci.* 1996; 85(10):1017–1025.
19. Pathan I.C. and Setty C.M. Chemical penetration enhancers for transdermal drug delivery systems. *Trop. J Pharm. Res*. 2009; 8(2): 173-179.
20. Castaneda P.S., Escobar-Chavez J.J., Aguado A.T., Cruz I.M.R. and Contreras L.M.M. Design and evaluation of a transdermal patch with atorvastatin. *Farmacia*. 2017; 65(6): 908-916.
21. Shehata T.M., Mohafez O.M.M. and Hanieh H.N. Pharmaceutical formulation and biochemical evaluation of atorvastatin transdermal patches. *Indian J. Pharm. Educ*. 2018; 52(1): 54-61.
22. Mahmoud M.O, Aboud H.M., Hassan A.H., Ali A.A. and Johnston T.P. Transdermal delivery of atorvastatin calcium from novel nanovesicular systems using polyethylene glycol fatty acid esters: Ameliorated effect without liver toxicity in poloxamer 407-induced hyperlipidemic rats. *J. Control. Release*. 2017; 254:10-22.
23. Subramanian S., Devi M.K., Rajesh C.V., Sakthi M., Suganya G. and Ravichandran S. Preparation, evaluation and optimization of atorvastatin nanosuspension incorporated transdermal patch. *Asian J. Pharm*. 2016; 10(4): 487-491.
24. Soujanya C., Prakash P.R. Formulation and *in vivo* evaluation of proniosomal gel based transdermal delivery of atorvastatin calcium. *Am. J. PharmTech Res.* 2018; 8(4): 156-172.
25. Immadi S., Allam K., Ampeti S., Modumpally A., Salpala R., Ampeti S. and More K. Improved absorption of atorvastatin prodrug by transdermal administration. *International journal of Biopharmaceutics.* 2011; 2(2): 54-56.
26. Thakkar H.P., Savsani H.G. and Srivastava P.K. Influence of inclusion complex and skin microporation on enhancement of transdermal permeation of raloxifene hydrochloride. *Indian J. Pharm. Sci*. 2019; 81(1): 22-31.
27. Kumar S.A., Debanth M., Rao S.J.V. New validated RP-HPLC analytical method for simultaneous estimation of atorvastatin and ezetimibe in bulk samples as well as tablet dosage forms by using PDA detector. *Curr. Drug Discov. Technol.* 2014; 11(4):259-70.
28. Apley M., Crist G.B., Fellner V., Gonzalez M.A., Hunter R.P., Martinez M.N., Messenheimner J.R., Modric S., Papich M.G., Parr A.F., Riviere J.E. and Marques R.C. Determination of thermodynamic solubility of active pharmaceutical ingredients for veterinary species: A new USP general Chapter. *Dissolution Technol.* 2017; Feb: 36-39.
29. Higuchi T., Connors K.A. Phase solubility techniques. *Advanced Analytical Chemistry of Instrumentation.* 1965; 4: 117-212.
30. Lv H.X., Zhang Z.H., Jiang H, Waddad A.Y. and Zhou J.P. Preapartion, Physicochemical characteristics and bioavailability studies of an atorvastatin hydroxypropyl-β-cyclodextrin complex. *Pharmazie*. 2012;67:46-53.
31. Galiullina L.F., Musabirova G.S., Latfullin I.A., Aganov A.V. and Klochkov V.V. Spatial structure of atorvastatin and its complex with model membrane in solution studied by NMR and theoretical calculations. *J. Mol. Struct.* 2018; 1167:69-77.
32. Kracun M., Kocijan A, Bastarda A, Grahek R., Plavec J. and Kocjan D. Isolation and structure determination of oxidative degradation products of atorvastatin. *J Pharmaceut. Biomed*. 2009; 50: 729-736.
33. Zhang HX, Wang JX, Zhang ZB, Le Y, Shen ZG and Chen JF. Microionization of atorvastatin calcium by antisolvent precipitation process. *Int J Pharm.* 2009; 374: 106-113.
34. Kim M.S., Jim S.J., Park H.J., Song H.S., Neubert R.H.H. and Hwang S.J. Preparation and characterization and *in vivo* evaluation of amorphous atorvastatin calcium

nanoparticles using supercrtical antisolvent (SAS) process. *Eur. J Pharm. Biopharm*. 2008; 69: 454-465.

35. Carvalho K.P., Rocha TC. and Leles MIG. Characterization of atorvastatin by TG and DSC. *Braz J. Therm. Anal*. 2012; 79-83.
36. Da Silva E.P., Pereira M.A.V., De Barros Lima F.P., Lima N.G.P.B., Barbosa E.G., Aragao C.F.S. and Bomes A. P.B. Compatibility study between atorvastatin and excipients using DSC and FTIR. *J Therm. Anal. Cal.* 2016; 123: 933-939.
37. Kong K., Zhu X., Metaleva E.S. and Su D.W. Physicochemical characteristics of the complexes of simvastatin and atorvastatin calcium with hydroxyporpyl-β- cyclodextrin produced by mechanochemical activation. *J Drug. Deliv. Sci. Technol*. 2018; 46: 436-445.
38. Kilian D., Lemmer H.J., Gerber M., du Preez J.L., du Plessis J. Exploratory data analysis of the dependencies between skin permeability, molecular weight and log P. Pharmazie. 2016; Jun;71(6):311-9.
39. Joshi H.N., Fakes M.G. and Serajuddin Abu T.M. Differentiation of 3-Hydroxy- 3- methylglutaryl- coenzyme A reductase inhibitors by their relative lipophilicity. *Pharm. Pharmacol. Commun*. 1999; 5: 269-271.
40. Sekkat N. and Guy R.H. Biological models to study skin permeation. In 'Pharmacokinetic optimization in drug research: Biological, physicochemical and computational strategies'. Eds. B. Testa, H. van de Waterbeemd, G. Folkers and R.H. Guy, Wiley-VHCA, Zurich, 2001, pp. 155-172.
41. Shimpi S., Chauhani B. and Shimpi P. Cyclodextrins: Application in different routes of drug administration. *Acta Pharm.* 2005; 55: 139–156.

تحضير ملح الآتورفاستاتين كولين ودراسة خصائصه الصيدلانية واحتمالية النفاذية عبر الجلد*

ربى الطراونة[1]، رندا منصور[2] دينا السبعاوي[1] و عماد حمدان[1]

1- كلية الصيدلة ، الجامعة الاردنية ، عمان ، الاردن.

2- كلية الصيدلة، جامعة فيلادلفيا ، عمان، الاردن.

ملخص

آتورفاستاتين كالسيوم مادة دوائية من مجموعة الستاتين مضادة لارتفاع الدهون في الجسم وتوافرها الحيوي قليل. ذكرت الدراسات السابقة طرقا لتحسين ذائبية الاتورفاستاتين. في هذه الدراسة تم تحضير الاتورفاستاتين على شكل ملح الكولين بغرض تحسين ذائبية الاتورفاستاتين وبالتالي تحسين قابلية الإمتصاص عبر الجلد. كذلك تم تحضير معقدات من ملح المنتج (اتورفاستاتين – كولين) مع الهيدروكسي بروبل بيتا سايكلوديكسترين. تم فحص الخصائص الصيدلانية للمواد المصنعة. تم في هذه الدراسة استخدام تقنية ثنائي الأبعاد لحسم الخلاف في تحديد الاشارات الخاصة للبروتونات في مادة الاتورفاستاتين وقد كان لذلك أثر كبير في فهم بناء الملح المتكون. وأظهرت النتائج المختلفة تكون ملح الكولين ومعقد الهيدروكسي بيتا سايكلودكسترين. كان للاتورفاستاتين كولين نتائج أفضل من حيث الذائبية بالمقارنة مع الاتورفاستاتين. كما تغير معامل توزع من 1.86للاتورفاستاتين الى 1.16 للاتورفاستاتين كولين. فكان لذلك أثر إيجابي على النفاذية عبر الجلد حيث كانت لملح الكولين أربعة أضعاف النفاذية للاتورفاستاتين. اما المعقد فلم يكن له تأثير إيجابي على النفاذية.

الكلمات الدالة: ستاتين، توافر حيوي، نفاذية عبر الجلد، معامل التوزع.

---

* تم إنجاز هذا البحث بدعم من عمادة البحث العلمي في الجامعة الأردنية.

تاريخ استلام البحث 2019/4/23 وتاريخ قبوله للنشر 2020/1/6.